Algal Research 75 (2023) 103266

Contents lists available at ScienceDirect

Algal Research

journal homepage: www.elsevier.com/locate/algal

Biotechnological investigation of *Pediastrum boryanum* and *Desmodesmus subspicatus* microalgae species for a potential application in bioenergy

Gislayne Santana Santos Jacinto [a], Glauber Cruz [b,*], Aluísio Alves Cabral [c], Glauco Vinicius Palhano Bezerra [c], Ramón R. Peña Garcia [d], Ulisses Nascimento Magalhães [e], Wolia Costa Gomes [a]

[a] *Postgraduate Program in Environment, Environmental Sciences Laboratory, Ceuma University, Rua Josué Montello 01 - Jd. Renascença II, 65075-120 São Luís, Maranhão, Brazil*

[b] *Processes and Thermal Systems Laboratory, Department of Mechanical Engineering, Federal University of Maranhão, Av. dos Portugueses 1966 - Bacanga, 65080-505 São Luís, Maranhão, Brazil*

[c] *Postgraduate Program in Materials Engineering, Department of Mechanics and Materials, Federal Institute of Education, Science and Technology of Maranhão, Av. Getúlio Vargas 04 - Monte Castelo, 65030-005 São Luís, Maranhão, Brazil*

[d] *Federal Rural University of Pernambuco, Academic Unit of Cabo de Santo Agostinho, Rua Cento e Sessenta e Três 300 - Cohab, 64049-550 Cabo de Santo Agostinho, Pernambuco, Brazil*

[e] *Postgraduate Program in Energy and Environment, Department of Technological Chemistry, Federal University of Maranhão, Av. dos Portugueses 1966 - Bacanga, 65080-505 São Luís, Maranhão, Brazil*

ARTICLE INFO

Keywords:
Biofuels
Biomass
Biotechnology
Cell growth
Physicochemical characterization
Thermal behavior

ABSTRACT

The production of photosynthetic microalgae is a promising ecological advantage for obtaining carbon credits. This paper addresses cultivation and preparation, growth analysis, physicochemical characterization (X-ray diffraction-XRD, Fourier transform infrared-FTIR, scanning electron microscopy-SEM, and energy dispersive spectroscopy-EDS), and thermal behavior (thermogravimetry-TG, derivative thermogravimetry-DTG, and differential scanning calorimetry-DSC) of two microalgae, namely *Pediastrum boryanum*-PB (CH007) and *Desmodesmus subspicatus*-DS (AEE431E) for a potential application as an energy resource. Regarding the former, the literature reports no specific study on the species, which shows high lipid productivity and fast growth. A synthetic culture medium (*Walter culture*-WC) was subjected to variations in pH, luminosity, and maximum growth reached in 12 and 13 days for PB and DS, respectively. TG/DTG curves identified the main thermal degradation stages, i.e., dehydration (DS (24.68–158.68 °C) and PB (20.06–116.18 °C)), devolatilization (DS (166.34–543.00 °C) and PB (128.22–493.93 °C)), and gasification or carbonization (DS (>550 °C) and PB (>500 °C)), and DSC curves revealed two endothermic events, an exothermic one for DS, and only one endothermic event and an exothermic one for PB. XRD patterns showed a cellulose crystallinity index (CI) for DS (22.54 %) and PB (28.82 %), confirming the predominance of amorphous regions. SEM images detected external epidermis for DS and some interconnected pores for PB. The FTIR spectra identified functional groups (lipids, proteins, and carbohydrates) and C═O, C—O, O—H, C—H, and C-O-C linkages, and EDS and ICP-OES identified the main organic, inorganic, and metallic elements. The microalgae species displayed characteristics similar to those of the other biomasses in the bioenergy industry, enabling their use in thermoconversion processes for biofuel production and considering some socioenvironmental aspects.

1. Introduction

Urbanization, industrialization, and excessive use of fossil fuels have increased greenhouse gases (GHG) in modern society [1]. On the other hand, the release of untreated wastewater threatens both human health and the environment, requiring the exploration of new, clean, renewable and sustainable energy resources [1]. As an example, some solid, liquid and/or gaseous resources have been used for the recovery and production of different biofuels, such as biodiesel, biomethane, biohydrogen, biooil and other products with high added value [2].

* Corresponding author.
E-mail address: cruz.glauber@ufma.br (G. Cruz).

https://doi.org/10.1016/j.algal.2023.103266
Received 9 June 2023; Received in revised form 11 September 2023; Accepted 16 September 2023
Available online 19 September 2023

In this context, microalgae have stood out as a promising biomass species for industrialization, since they cause no harmful effects to the environment [3]. Although the production of biofuels from biomass is not a new concept, it has been more frequently investigated due to the increasing demands and constant increases in the prices of fossil fuels [3]. The production of biofuels with microalgae has faced several challenges, such as energy deficiency and costly processes for growing and harvesting a substantial amount of necessary nutrients, (e.g., nitrogen (N) and phosphorus (P)) using conventional methods of cultivation [3].

Interestingly, integrated membrane systems of these microorganisms are possible alternatives not only for the cultivation and harvesting of microalgae, but also for the production and recovery of biofuels and other products with high added value [4]. As an example, the growth and cultivation of microalgae require special attention, since they can lead to the creation of a socioeconomically and environmentally correct organization as a way of producing biofuels from different species of microalgae [5].

Brazil is a country of continental dimensions and rich in water resources, such as the Amazon River, and the choice of freshwater microalgae species for the biofuel production meets the need for information, including low cost in cultivation, ease of adaptation to the culture environment, high growth rate, CO_2 fixation, high levels of carbon and oxygen, higher heating value, and low contents of nitrogen, sulfur, and ash [6]. The Brazilian Northeast shows an influential and important coastal extension with a great diversity of marine species, including different microalgae, such as *Pediastrum boryanum* - CH007 and *Desmodesmus subspicatus* - AEE431E [7]. Maranhão State, especially São Luís city - Latitude: 2°31′51″ South and Longitude: 44°18′24″ North, requires new possibilities for the production of different biomasses with the following main characteristics: cultivation with no direct confrontation with food production, devastation of areas of fertile soil (export-type agriculture), and consumption of large volumes of clean freshwater [7].

Microalgae are photosynthetic organisms with a great diversity of microorganisms regarding their morphology, complexity degree, and size [8,9]. Freshwater microalgae of *Pediastrum* genus belong to the *Eukaryotic* domain, Protista kingdom, *Chlorophyta* division (green algae), *Chlorophyceae* class, *Sphaeropleales* order, and *Hydrodictyaceae* family [10], whereas microalgae *Desmodesmus* are commonly found in freshwater and less frequent in salt water, i.e., they are *chlorophyllous* microorganisms with a unicellular structure [11]. *Desmodesmus* and *Scenedesmus* are included in the *Chlorophyceae* class, *Sphaeropleales* order, and *Scenedesmaceae* family [12].

Microalgae have acquired significant importance as a possible source of sustainable feedstock for the biofuels production. Among several species reported in the literature (e.g., *Chlorella sorokiniana* SDEC-18 [13], *Botryococcus braunii* [14], *Anabaena Arthrospira fusiformis*, *Arthrospira platensis*, *Chlorella vulgaris*, *Chlorella sorokiniana*, among the 38 species in this study [15], *Tribonema* sp. [16]) can accumulate lipids inside, which can be extracted and converted directly into biodiesel by thermochemical, biological, or biochemical processes.

Pediastrum boryanum - CH007 and *Desmodesmus subspicatus* - AEE431E require solar energy, carbon dioxide (CO_2), and some nutrients to produce bio-oil more efficiently compared to traditional oilseed crops such as soybean, sunflower, and olive [17]. Therefore, their use in real production processes is an important justification for minimizing the harm caused by global warming due to the burning of fossil fuels.

Microalgae offer other advantages over conventional oilseeds, such as fast life cycle and continuous production throughout the year and exponential growth under cultivation without socioenvironmental damage and lower consumption of freshwater compared to traditional plantation crops. After extraction, the biomass can be used in animal feed and as organic fertilizer, source of dyes, and natural antioxidant [18,19]. Another modern and technological application for microalgae concerns bioremediation programs [5,7], or production of medicines and drugs, food and chemical intermediates for the petrochemical sector, bioplastics, biokerosene, and various bioactive compounds [7,20].

This article analyzes the cultivation and, from a biotechnological point of view, the growth curve and the physicochemical characterization and thermal behavior of *Pediastrum boryanum* - CH007 and *Desmodesmus subspicatus* - AEE431E, as two potential candidates for bioenergetic application through thermochemical processes in specific equipment such as Drop Tube Furnace (DTF).

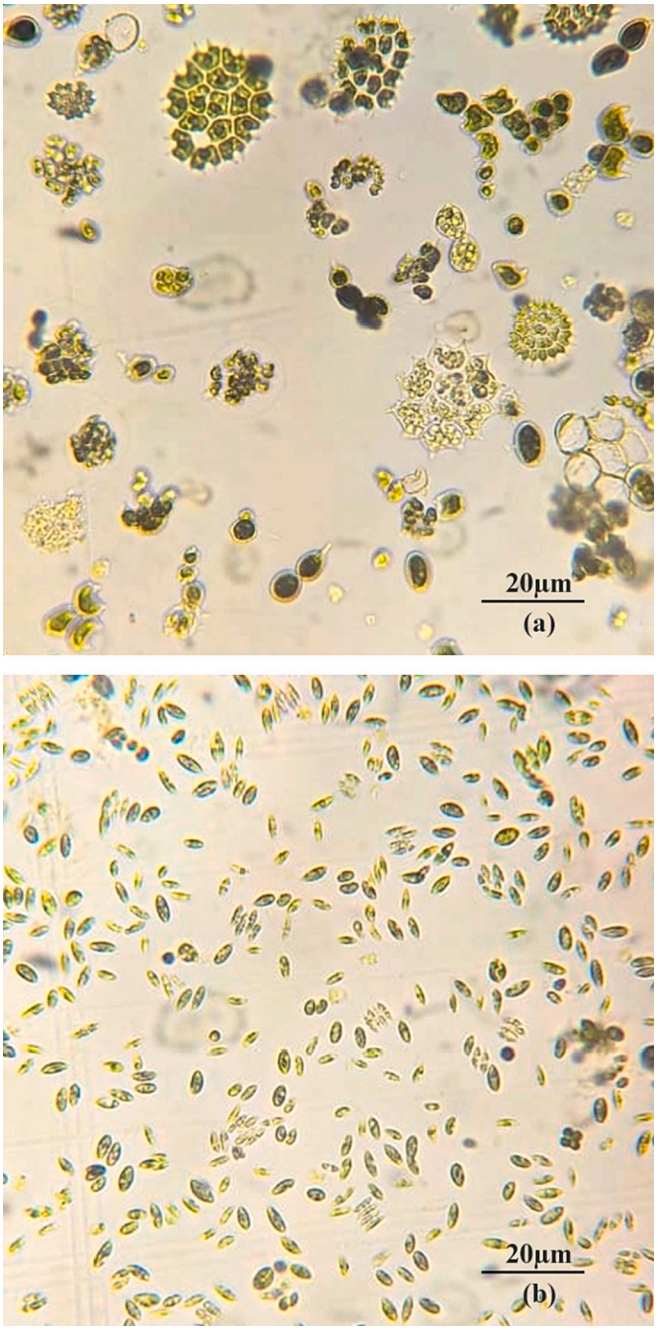

Fig. 1. Optical microscopic images of (a) *Pediastrum boryanum* and (b) *Desmodesmus subspicatus* microalgae, with a magnitude of 40×.

2. Materials and methods

2.1. Cultivation systems of microalgae

2.1.1. Microalgae species studies

Strains of *Pediastrum boryanum* - CH007 (Fig. 1a) were chosen for optimizing the cultivation system. They were kindly donated by the Freshwater Microalgae Cultivation Bank (BCMD) of the Microalgae Laboratory (LM) of the Institute of Biological Sciences (ICB) at Federal University of Rio Grande (UFRG), since the literature reports no other more specific studies, due to the high productivity rates of lipid contents and rapid growth [20] for the biomass production, favoring the generation of biofuels. *Desmodesmus subspicatus* - AEE431E (Fig. 1b), National System for the Management of Genetic Heritage and Associated Traditional Knowledge (SisGen) at Federal University of São Carlos (UFSCar), another more frequently studied species, was used for comparative purposes.

Fig. 1a shows the formation of discoid colonies with cells arranged in concentric circles in the peripheral cells' incisions or 1-2-4 apophyses (tapered extensions) and Fig. 1b displays colonial individuals with two, four, eight, sixteen, and up to thirty-two cells within the coenobium, i.e., a more common feature among green algae, which float on water surfaces.

2.1.2. Preparation of the synthetic cultivation medium

WC (*Walter Culture*) was used as the synthetic cultivation medium. It underwent a small adaptation, i.e., calculations were performed adjusting the laboratory glassware and transforming kilogram (kg) measurement unit to milliliter (mL) [21]. Its pH (potential hydrogen) was maintained as ≈7.0 and its composition is shown in Table S.1 (see supplementary material).

Stock solutions (standard and initial ones) were prepared with the aid of analytical scales (M214-AIH) for the weighing of the reagents and stored in a laboratory refrigerator (Consul, Cycle Defrost Duplex CRD37EB) at ≈20 °C average temperature. Except the vitamin's solution, which was sterilized through filters of 0.22 μm average pores for avoiding thermal degradation, the solutions were autoclaved at 0.5 atm average pressure and ≈120 °C towards avoiding biological contamination [22].

2.1.3. Climatization of the microalgae cultivations

The culture media were acclimatized to a favorable environment to optimize the growth of *Pediastrum boryanum* and *Desmodesmus subspicatus*, whose cultures were developed in 2000 mL Erlenmeyres used as experimental bench photobioreactors and incubated at (23 ± 2) °C, with agitation by directed injection of compressed air (model AC 202–240 V at 3 L min^{-1} flow rate) to ensure a better homogenization. The fluorescent lamps of the experimental apparatus provided an average power of 2000 Lux for DS and 3000 Lux for PB, controlled by a Kasvi Benchtop pHmeter (model K39-2014B Benchtop pHmeter, pH 0–14, 220 V).

2.1.4. Determination of the experimental parameters for the microalgae

2.1.4.1. Microalgae growth. An optical microscope (40×) determined the growth of the two microalgae through an evaluation of their cellular density in function of the cultivation time in each experimental unit. The samples were removed every 24 h after the start of the cultivations for the cell counting in a *Neubauer* chamber (K5-0011 - KASVI) so that the cellular density, expressed in terms of number of cells per milliliter of the cultivation medium (cells mL^{-1}), could be determined.

The cells were counted in triplicate ($n = 3$) for better reproductability and experimental reliability. The number of cells corresponds to the arithmetic average of the three countings [23]. The cultivation time was expressed by number of days elapsed from the start of the inoculation (adaptation period - *lag phase*) to the cellular density maximum reach (stationary phase). The dispersion graphs, where *x-axis* indicates cultivation time [days] and *y-axis* denotes number of cells [mL^{-1}], represented the growth curves of *Pediastrum boryanum* and *Desmodesmus subspicatus* samples.

2.1.4.2. Production and characterization of the dry microalgae biomass. 2 L Erlenmey flasks and distilled/autoclaved water at 121 °C for 15 min were used for the preparation of the inoculum. The number of replicates for the process was 50 times for each sample throughout the microalgae cultivation. Under aseptic conditions, 1800 mL of culture medium were transferred to flasks to which 100 mL of suspension of *Pediastrum boryanum* and *Desmodesmus subspicatus* were added. After reaching the steady state of cell growth, the biomass was separated by a flocculation process with aluminum sulfate ($Al_2(SO_4).H_2O$) at 5.0 % concentration [24,25]. The supernatant (biomass) was separated by centrifugation.

After the flocculant addition, the solution was neutralized with the formation of sedimented flakes, which were gradually removed - the material was concentrated in the lower part of the bench photobioreactor [25]. The sedimentation process took place over 12 h (rest time of the microalgae). The cultivation microalgae slurry was then transferred to 50 mL Falcon tubes, which were taken to a digital centrifuge (*Model CT-4000*), where the samples were subject to a 2000 rpm rotation for 7 min and the supernatant was separated from the microalgae biomass. At the end of the process, the total wet biomass was placed in the inferior part of a Petri plate and the produced biomass was dried in a sterilization oven (7 Lab. model SSAi 40 L inox) and exposed to 60 °C for 48 h for the obtaining of a dry biomass sample [26].

2.1.4.3. Statistical analysis of the growth curve. Data on microalgae growth under the conditions described were evaluated by Analysis of Variance (ANOVA), with $n = 3$ sample size for each species.

The test was conducted at a 5.0 % significance interval and data were submitted to *Tukey* test for a normal distribution analysis (distribution is considered normal for $p > 0.05$). All data used in this study were considered homogeneous and normal [27].

After the preparation of the inoculum, the volume of the two dry biomasses obtained was sufficient for their productivity analysis by physicochemical characterizations and thermal behavior, as addressed in what follows.

2.1.4.4. Fourier transform infrared spectroscopy (FTIR). The infrared spectra of the samples were obtained in the 4000 to 400 cm^{-1} spectral region, in transmittance mode with 4 cm^{-1} variation in a spectrophotometer (*Shimadzu, IR-Prestige-21*).

2.1.4.5. Thermal analysis (TG/DTG/DSC curves). The TG/DTG/DSC curves for *Pediastrum boryanum* and *Desmodesmus subspicatus* were measured in a simultaneous thermogravimetric analyzer (NETZSCH STA 449C) under non-isothermal conditions. Approximately 10 mg (±0.5) of each sample were inserted in a platinum crucible under inert atmosphere (argon 5.0) with 50 mL min^{-1} flow rate. The samples were heated from room temperature (≈25 °C) to 800 °C, at 10 °C min^{-1} heating rate (β) and Proteus® software was employed for the analyses of the curves. The instrument had been previously calibrated with $RbNO_3$, $KClO_4$, CsCl, K_2CrO_4, and $BaCO_3$ pure compounds.

2.1.4.6. Scanning electron microscopy (SEM images) and energy dispersive spectroscopy (EDS). SEM images were obtained under a Scanning Electron Microscope (*TESCAN*, *VEGA3*) corresponding to a tungsten thermionic emission system, whereas the dispersive energy spectra were acquired by an energy dispersive spectroscopy detector by X-ray (EDS) coupled to the SEM (*Oxford, 51-ADD0048*).

2.1.4.7. X-ray diffraction (XRD). X-ray diffraction patterns were obtained in a diffractometer (*Creator Version*) with CuKα radiation (λ =

1.541 Å, 40 kV - 40 mA) and powder diffraction configuration.

The crystallinity index of cellulose (CI) was calculated by Eq. (1) [28], where I_{002} is the crystalline region intensity and I_{am} is the amorphous region intensity, both present in the samples studied.

$$IC\% = \frac{(I_{002} - I_{am})*100}{I_{002}} \quad (1)$$

2.1.4.8. Inductively coupled plasm optical emission spectrometer (ICP - OES). The concentration of the main inorganic and mettalic elements in *Pediastrum boryanum* and *Desmodesmus subspicatus* was determined by an Optical Emission Spectrometer by Inductively Coupled Plasm (*Varian, ICP - OES 710ES*).

2.1.4.9. Calorimetry analysis (HHV). The Higher Heating Value [MJ kg^{-1}] was determined according to ASTM E711 standard [29] and using a bomb calorimeter (*IKA-C200 Calorimeter*, USA) with 0.5 g sample mass. The analysis was performed in duplicate for a better reprodutibility.

3. Results and discussion

3.1. Total concentration of algae

The reference values for the determination of the microalgae concentration at the beginning of the experiments were based on *Actinastrum hantzshii* microalgae cultivated in the control medium (WC) with 43×10^5 cell mL^{-1} cellular density [23,27,30]. After cultivation, the two microalgae studied were counted microscopically daily, with the aid of a Newbauer camera. As the days passed, the cells multiplied, absorbing the nutrients provided by the medium and identifying the phases with their respective cells number, namely lag phase, growth-acceleration phase, exponential growth phase, stationary phase, and death phase. The previously found reference values were compared with data from the literature, i.e., the total cells for *Pediastrum boryanum* and *Desmodesmus subspicatus* were 42×10^5 cells mL^{-1} and 46×10^5 cells mL^{-1}, respectively.

3.2. Determination of cellular counting per growth phase

Towards the algae growth follow-up, the samples monitored by their pH were placed in eppendorfs containing 1.0 mL and fixed in acetic lugol at 5.0 %.

The procedure was checked in 12 days for *Pediastrum boryanum* and 13 days for *Desmodesmus subspicatus* in all cultivation media employed, considering the life cycles of such microorganisms in the control medium, as shown in Fig. 2(a–b).

Fig. 2(a–b) shows some distinct phases during the microalgae growth phases, namely lag, growth-acceleration, exponential growth, stationary, and death.

(I) ***Lag phase***: the cellular quantity for the two species was 2×10^5 cells mL^{-1}, demonstrating their adaptation to the new cultivation medium (WC) under the same conditions of the original solution. The microalgae synthesized the enzymes necessary for the metabolism of the components present in the cultivation medium [31]. According to Suzana et al. [32], WC, commonly used for the cultivation of some microalgae species, provides nutrients required for their development, contributing to good productivity and an adequate cellular composition for the obtaining of byproducts of industrial interest (biofuels, bioethanol, and/or biomethane).

(II) **Growth-acceleration phase**: from the 2nd to the 4th day (≈38×10^5 cells mL^{-1}), *Pediastrum boryanum* (PB) startet growing. At the beginning of the phase, the cells were adapted to the medium and began to multiply. The end of the phase was marked, since all microorganisms showed a simultaneous multiplication [33]. Such a phase was observed from the 2nd to the 10th day of the experiments for *Desmodesmus subspicatus* and characterized by an exponential cellular increase (≈30×10^5 cells mL^{-1}), i.e., a large production of proteins and/or enzymes and a high DNA replication rate DNA [34].

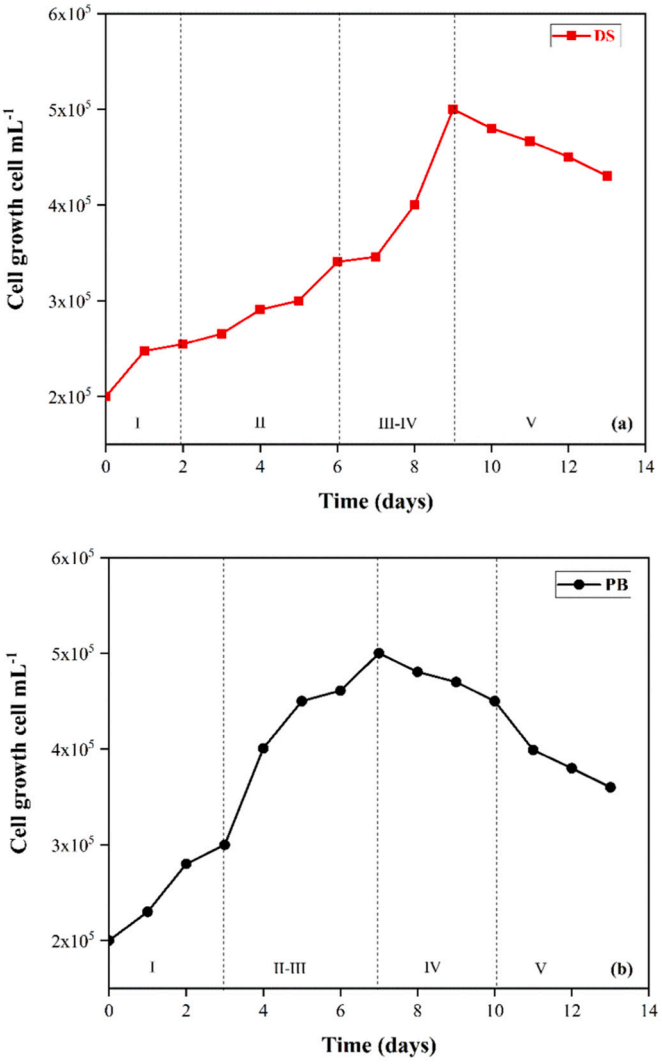

Fig. 2. Daily follow-up of the cellular counting and growth phases for (a) *Desmodesmus subspicatus* (DS) and (b) *Pediastrum boryanum* (PB).

(III) **Exponential growth phase**: from the 7th day for PB, with ≈51×10^5 cells mL^{-1}, and from the 11th day for DS, with ≈50×10^5 cells mL^{-1}. This phase describes the occurrence of a specific maximum growth rate held constant until the end. The end of the phase is determined by the end of the maximum growth rate. The phase does not show a shortage or deficiency of nutrients or their transport to the microalgae [35].

(IV) **Stationary phase**: from the 8th and 10th days, 45×10^5 cells mL^{-1} were presented for PB and 52×10^5 cells mL^{-1} were shown for DS in the 11th day. The phase is marked by the depletion of one or more nutrients; therefore, the growth rate equals the death one, i.e., the microalgae concentration is kept practically constant. An adequate nutrition of the microalgae requires nutrients reservations or an autolysis suffered by some cells, releasing their nutrients for meeting the nutritional needs of the other cells [31]. However, a short period of time between the 10th and the 14th days was comprehended for the DS sample. The medium composition underwent some changes due to either the

production of metabolites, or the depletion of essential nutrients, leading to a reduction in the progressive growth rate of the cells, which then entered a stagnation phase. Under new conditions, they showed a slow growth, declining after some days [32].

(V) **Death phase**: occurred between the 11th and the 13th days with PB, whose cells varied between 38×10^5 and 36×10^5 cells mL^{-1}, respectively. Their death was caused by the depletion of the nutrients in the culture medium of the microorganisms. An autolysis, or disruption of the microorganisms, occurred by the action of intracellular enzymes [31]. Regarding DS, the cultivation of that microalgae showed no decline phase, since the cells were collected during the establishment of the stationary phase, when the cells are fully formed, stabilized, and with interesting quantities for collect and development of specific analyses [36].

In comparison to the growth of PB and DS in this study, Chiranjeevi and Venkata [37] evaluated the productivity of *Chlorella vulgaris* and *Scenedesmus obliquus* microalgae cultivated in effluents of fish viscera (liquid/solid effluents from the fish production and slaughtering and domestic wastes (including washing and cleaning water from daily processes)), obtaining a good yield for both species. Despite *Scenedesmus obliquus,* cellular growths of 120×10^5 cells mL^{-1} in viscera effluents and 250×10^5 cells mL^{-1} in domestic wastes were observed.

3.3. Statistical analysis of growth curves

ANOVA, with 95.0 % reliability, was conducted with data from the growth curves of DS and PB (Fig. 3). The results showed the number of grown cells, indicating excellent growth responses and a good biomass production in the benchtop bioreactor as the alternative medium used, suggesting it can be safely employed for the obtaining of microalgae biomass in multiple applications [38].

A high positive linear correlation was observed with the data of variables of the growth curves the determination coefficients (R^2) were 0.9420 and 0.9753 for *Pediastrum boryanum* and *Desmodesmus subspicatus*, respectively. The results enabled the obtaining of equations of linear and polinomial regressions of 4rd-order between the two variables for each culture [39].

However, ANOVA was conducted for the choice of factors that showed statistical significance in the biomass process [39]. *F* (ratio of variance) showed significant differences between the averages of the factors studied and *p*-value (probability of significance), denoting a high reliability degree in the results [40]. Regarding the present study, the higher the *F* values calculated, the more significant the factors for the process. As an example, the high values reported for the ratio of variance ($F = 433.71$) for *Desmodesmus subspicatus* and low *p*-value ($p = 3.46 \times 10^{-5}$), confirming the significance level adopted ($p < 0.05$) and for *Pediastrum boryanum* ($F = 32.50$) and *p*-value ($p = 5.38 \times 10^{-5}$) indicated the lower the *p*-value, the higher the reliability degree [41]. The results showed 5.0 % significance factors, which may be justified by the presence of mineral salts in the WC cultivation medium that are aggregated in the biomass and do not correspond purely to the microalgae biomass [42]. The result is also related to the correlation matrix, according to which the productivity for both microalgae showed no significant correlation with the other parameters evaluated [39–42].

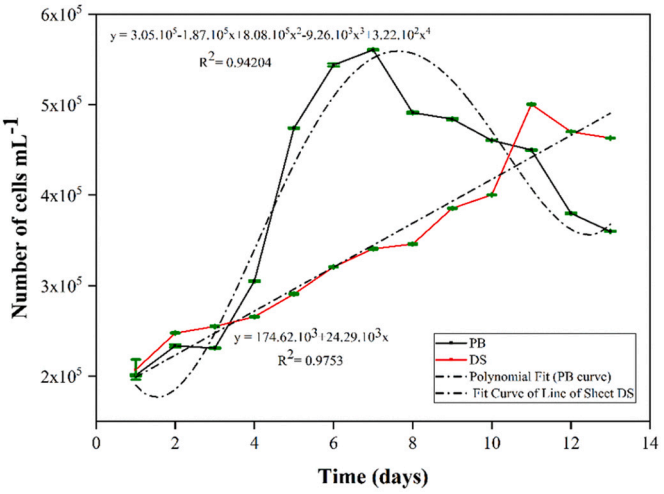

Fig. 3. Linear and polynomial mathematical models of adjustments for the growth curves of *Desmodesmus subspicatus* (PB) and *Pediastrum boryanum* (DS).

3.4. Fourier transform infrared spectroscopy (FTIR)

Fig. 4 shows the main absorption groups in the infrared region for the two microalgae species (see also Table S.2) [43].

According to Shu-Yuan et al. [43], the FTIR spectra of *Chlorella sorokiniana* microalgae, whose proteins are characterized by two strong bands at around 1645 and 1540 cm^{-1}, are associated with the stretching mode of C═O bond and a combination of the deformation of N—H bond and C—N stretching of the complex amide vibrations, respectively [44]. Two strong bands characterize the presence of lipids: (i) stretching CH_2 and CH_3 bands at the 2850–3000 cm^{-1} region and; (ii) C═O vibration modes associated with the lateral chain of the ester carbonyl group at 1740 cm^{-1} [45]. The bands at 1000–1250 cm^{-1} correspond to vibrations of carbohydrates and phospholipids [45].

In this study, the FTIR analyses identified some functional groups, such as carboxyl, amine, hydroxyl, carbonyl, among others. Sepctra are related to presence of humic acids (main organic component of several water bodies, dystrophic lakes, and oceans), which are relatively simple and show few absorption bands [46].

Mainly lipids, proteins, and sugars were attributed to the two microalgae species. According to Thomas et al. [47], a slight displacement of the FTIR bands towards the shorter wavelengths was observed. The main bands for all samples in the present study were around 3600–3000 cm^{-1}, which are strong characteristics of hydroxyl (OH) vibration modes (OH) [48].

The spectra of *Desmodesmus subspicatus* and *Pediastrum boryanum* showed high similarity to those of *Spirulina platensis* [49]. Bataller and Capareda [50] reported both spectra of the biomasses showed an amide I band resulting from the C—O stretching vibrations of peptide bonds observed between 1774 and 1583 cm^{-1}. Amide II band, which results in

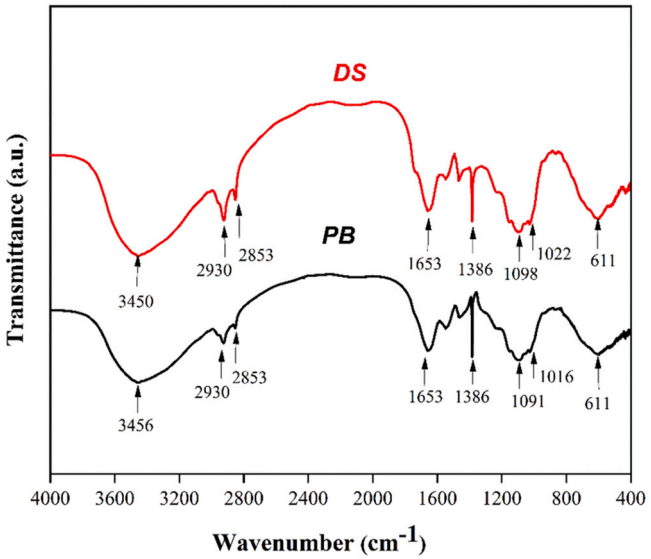

Fig. 4. FTIR spectra for *Desmodesmus subspicatus* (DS) and *Pediastrum boryanum* (PB).

C═O linkage, and N stretching vibrations are observed between 1583 and 1484 cm^{-1}. The lateral chain of COO– protein and the complex amide III band are present, respectively, at 1426–1377 cm^{-1} and 1329–1290 cm^{-1} [50].

Radical O—H (alcohols and phenols), which corresponds to vibrational stretching, can be observed in the wavelength between 3960 and 3340 cm^{-1}, whereas C—H (alkanes) is present between 2981 and 2767 cm^{-1} [51]. C—O stretching is present at 1762–1719 cm^{-1} and a deformation combination band O-CH and C-OH is observed between 1560 and 1350 cm^{-1}. For example, Bataller and Capareda [50] studied *Spirulina platensis* microalgae species and stated that C—H (single, double, or triple bonds) and O—H (single bonds) deformations are present between 1186 and 1350 cm^{-1} [52]. The characteristic bands of carbohydrates (C-O-C) and C stretching were observed at 955–1186 cm^{-1}, and the absorption bands (CH_3 and CH_2) are at 2998–2829 cm^{-1}. Those characteristics of lipids and C—O ester absorption can be observed at 1771–1688 cm^{-1}, although little evident, probably due to the low absorbance or the low lipids contents and superposition with the amide I band tail (i.e., they determine the minimum amount of biomass required for the production of homogeneous films with a good signal/noise ratio with no bands saturation) [49]. C—O stretching is present at 1211–1139 cm^{-1} and CH_2 absorption bands are observed at 1482–1456 cm^{-1} [50].

3.5. Thermal analysis (TG/DTG curves)

Fig. 5 shows the TG/DTG curves for (a) *Desmodesmus subspicatus* (DS) and (b) *Pediastrum boryanum* (PB), both with 3 (three) main thermal degradation events.

Regarding DS species, the first stage (I) is associated with a small mass loss due to the dehydration or evaporation of moisture (water at intracellular level). The second stage (II) represents the main devolatilization reactions, in which most of the sample mass was lost or released as volatile materials associated with the thermal degradation of carbohydrates, polysaccharides, proteins, and lipids [53,54]. The outer cell wall of microalgae generally contains specific polysaccharides, such as pectin, agar, and alginates [55]. On the other hand, the inner cell wall is composed mainly of cellulose and organized into layers of fibers that offer resistance and flexibility to the structures [56]. Although it is a hydrophilic molecule, cellulose is completely insoluble in water due to its large size, so that the molecule requires high temperatures for its breakdown [57]. A "shoulder" appears in the DTG curve at approximately 280.0 °C, which may be attributed to the thermal degradation of proteins and polysaccharides soluble at low temperatures [58]. Near 310.0 °C, another "shoulder" appears in the second stage, which may be attributed to the thermal degradation of holocellulose (cellulose + hemicellulose together) on the cell wall [59,60]. Finally, the third stage (III) is represented by high temperatures and associated with the total decomposition of all organic matter and some inorganic elements contained in the microalgae species [26,61].

Regarding *Desmodesmus subspicatus*, event (I) ranged between 32.0 and 163.0 °C and corresponds to the dehydration or evaporation process due to the presence of free water and/or water weakly bonded to biomolecules; however, for *Pediastrum boryanum*, the event occurred between 37.0 and 175.0 °C. Such a temperture change can be evidence PB released a smaller quantity of intrinsic moisture [62], or showed a low boiling point [63]. Stage II, with 163.0–317.0 °C to 174.0–324.0 °C temperatures for DS and PB, respectively, can be associated to the devolatization process, including depolymerization and decarboxylation, which are attributed mainly to the thermal decomposition of carbohydrates and proteins [64]. Such reactions are the major events of mass loss in microalgae, especially because those two components are found in large quantities in different microalgae species, mainly concerning carbohydrates [65]. Stage III (in the 317.0–601.0 °C and 324.0–599.0 °C range for DS and PB) can be associated with the thermal decomposition of the remaining organic compounds and some inorganic and metallic ones, which may occur as gasification products, and to the formation of compounds based on carbon and/or non-volatile elements that evaporate at high temperatures, forming CO gases (carbon monoxide) and CO_2 (carbon dioxide) [61].

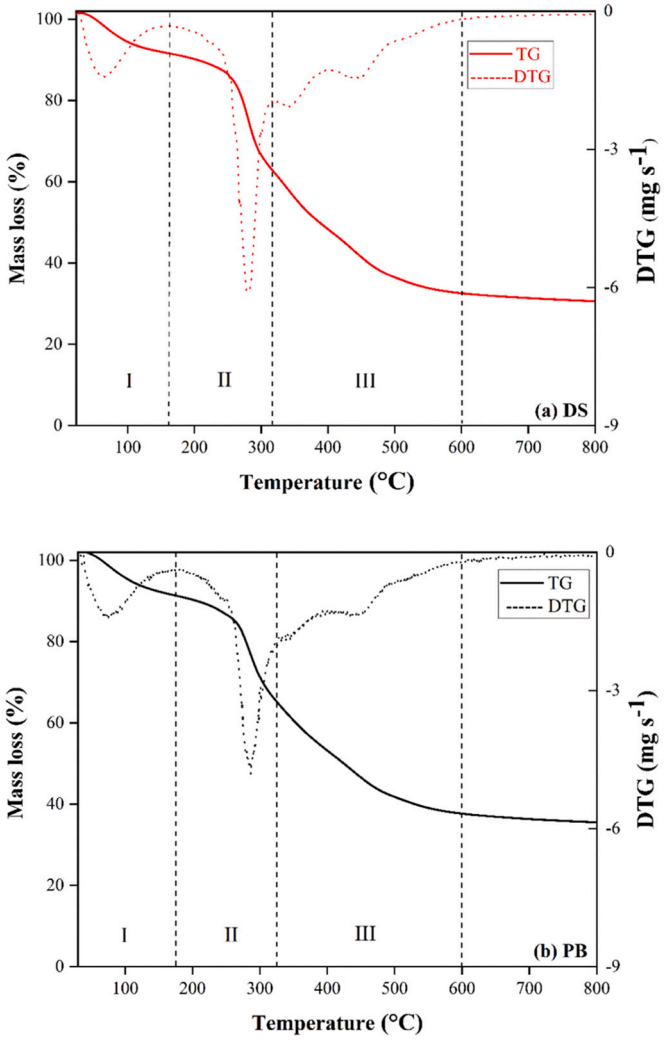

Fig. 5. TG/DTG curves: (a) *Desmodesmus subspicatus* (DS) and (b) *Pediastrum boryanum* (PB) under inert atmosphere (argon 5.0), 10 °C min^{-1} heating ratio, and room temperature up to 800 °C.

As an example, for *Botryococcus braunii* microalgae and in comparison to this study, the TG/DTG curves were divided into three distinct regions, indicating the three main thermal decomposition stages [63]. The first (I) was the evaporation of both moisture and organic compounds of low boiling point at ≤156.0 °C, i.e., according to the heating rates applied. The chlorophyll decomposition (*Clorofila clorobium*) may also have occurred at 80.0–110.0 °C, since chlorophyll is an unstable compound and can be easily degraded at temperatures between 80.0 and 145.0 °C [66]. However, the thermal decomposition of chlorophyll in that stage for *Botryococcus braunii* produced no compounds, such as phytane and pristane, some chlorophyll species commonly found in microalgae [67]. Phase II of degradation occurred from 156.0 to 557.0 °C, with a thermal decomposition of different condensable and non-condensable volatile materials, depolymerization, decarboxylation, and breakage of carbohydrates, proteins, chlorophyll, and lipidic compounds present in microalgae [68]. Interestingly, some carbohydrates and proteins can be decomposed at, respectively, 200.0 to 300.0 °C and 280.0–400.0 °C [69]. However, the lipids present in the microalgae of this study were thermally degraded at 315.0 to 600.0 °C.

The DTG curves showed more prominent peaks during

devolatization stages or maximum decomposition rates, indicating a thermal degradation of the main chemical constituents present in the different samples of microalgae species [70]. The first less intense peak for DS (≈30.0–160.0 °C) and PB (≈36.0–175.0 °C) represented a thermal decomposition of proteins and carbohydrates, whereas the second more pronounced peak of the aforementioned samples (≈250.0–316.0 °C; ≈263.0–326.0 °C) can be associated with the thermal decomposition of lipids or other fatty acid-based compounds [65]. In stage III, the DTG curve revealed the last thermal decomposition started at ≈317.0–600.0 °C (for both samples). The thermal degradation of the compounds present in stage III was confirmed to be due to gasification and formation of non-volatile carbon compounds that evaporated towards forming gases such as CO and CO_2 at high temperatures [65].

3.6. Differential scanning calorimetry (DSC curves)

Fig. 6 shows the DSC curve of *Desmodesmus subspicatus* (DS) and *Pediastrum boryanum* (PB).

Fig. 6 displays a protein denaturation transition inversely related to the water content and an endothermal tendency (decomposition product) [71]. *Desmodesmus subspicatus* clearly showed three endothermal events for the three stages, with 51.1 °C, 268.1 °C, and 422.3 °C peak tempertures, respectively, as also observed by You and Xiaojie [72], simultaneously associated with TG and DTG curves [73].

However, *Pediastrum boryanum* showed only one exothermic event in stage II, with 272.9 °C peak temperature, and three endothermal events with 58.9 °C, 420.6 °C, and 507.3 °C peak temperatures, correlated directy with TG/DTG curves, respectively [74].

Protein denaturation is characterized by the thermal cracking of hydrogen bonds, exposing the main hydrophobic groups, attracted towards forming disulfide-type crossed bonds, which form networks/meshes that retain water and form the gel [75]. The three endothermal events for *Pediastrum boryanum* in this study were related to protein denaturation [71].

On the other hand, the thermal degradation of some vegetable oils produces some volatile compounds such as fatty acids, aldehydes, and alcohols as secondary products and some compouds such as polycyclic aromatic hydrocarbon and acrylamide, which may exert several effects on human, animal, and plant health, since they are toxic and display some carcinogenic and mutagenic properties [76].

3.7. Scanning electron microscopy (SEM images)

Fig. 7(a–d) shows an image obtained by Scanning Electron Microscopy (SEM images) for *Desmodesmus subspicatus* (Fig. 7a–b) and *Pediastrum boryanum* (Fig. 7c–d). The technique also determined the main morphological differences, structural or textural effects for the two studied samples through images with different amplitudes [77].

Fig. 7(a–b) displays the formation of more heterogeneous morphological surfaces in *Desmodesmus subspicatus*, with different and irregular pore sizes [32] in comparison to *Pediastrum boryanum*. Yu et al. [28] studied the application of vegetable coals obtained by the pyrolysis of *Chlorella vulgaris* microalgae species in biorefineries and reported such a porous and irregular structure formed on the surface of the samples might contain active sites of bond, favoring the application of *biochar* produced as a biological adsorbent for soil tretament. It would promote fertilization for increasing the water retention capacity with molecules of gases and liquids of other substances retained on the surface of the samples. *Desmodesmus subspicatus* (Fig. 7a–b) frequently showed the presence of several external epidermis of different sizes on the cells and cellular walls [62,77].

The samples showed a rigid cellular wall, with formation of granulations with one or more cells and whose size ranged from 4.8 to 12.0 μm length and 2.8–7.3 μm width [78].

However, according to the micrograph in Fig. 7(c–d), the morphology of *Pediastrum boryanum* (PB) was highly irregular and rigid, with particles agglomerates of several sizes on the surface and some interconnected pores of different shapes and sizes [79].

Breil et al. [80] claimed some microalgae species, such as *Spirullina,* show phenotypic plasticity, i.e., capacity to alter their own physiology or morphology in response to the environment and/or conditions under

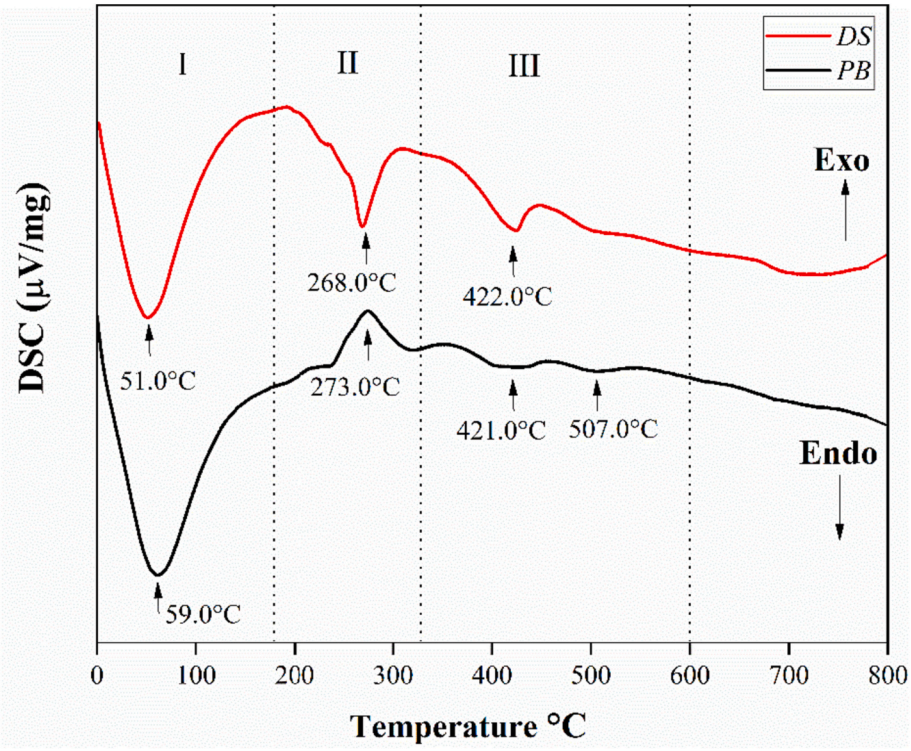

Fig. 6. Differential scanning calorimetry (DSC curves) for *Desmodesmus subspicatus* (DS) and *Pediastrum boryanum* (PB).

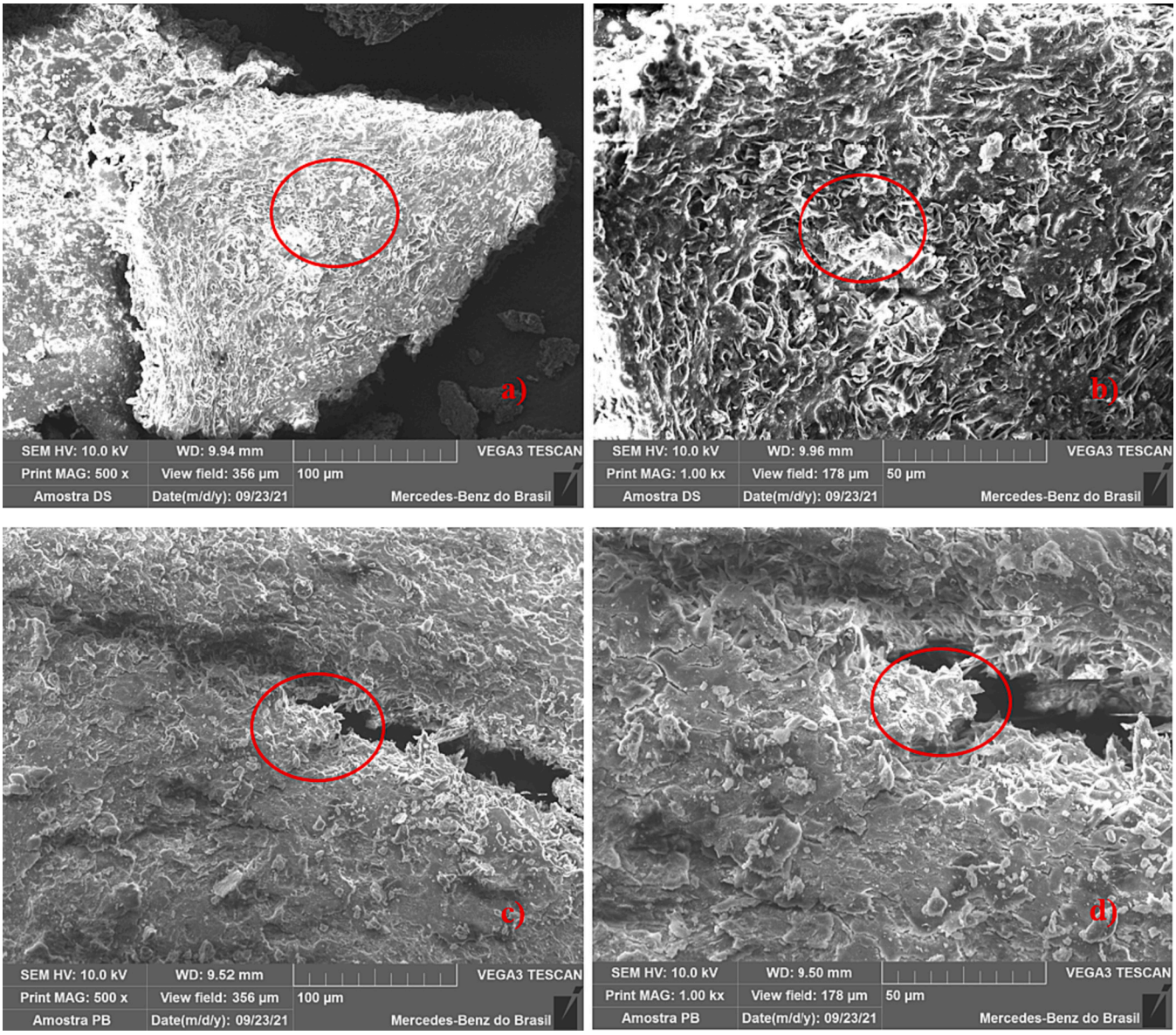

Fig. 7. SEM micrographs of *Desmodesmus subspicatus* (DS): (a) 500× and (b) 1000× and *Pediastrum boryanum* (PB): (c) 500× and (d) 1000×.

which they live, namely luminous intensity, temperature and/or availability of nutrients. The authors reported some morphological alterations in *Desmodesmus subspicatus* are related to the availability of nutrients, leading to the formation of colonies in low concentrations of nutrients and unicellular formation in high amounts of nitrogen and phosphor [77,80].

The structural morphology of the two microalgae species will be fundamental for validating other physical properties (e.g., porosity, rigidity, size, and grains contour). Therefore, both shape and size of the particles directly affect different thermal processes, flow fluidity, heat and mass transfer areas during thermochemical processes, probably due to the retention of gases in the pores [62].

Despite the different compositions of the culture media, the comparative results of the SEM images of the microalgae showed the morphological differences of the cells and/or cellular walls of the two species were not significant.

3.8. Energy dispersive spectroscopy (EDS)

Fig. 8 diplays the contribution of Energy Dispersive Spectroscopy to determine the composition of the main inorganic elements and alkaline metals present in the dry biomass of *Desmodesmus subspicatus* (DS) and *Pediastrum boryanum* (PB).

The transformation of microalgae into biofuels requires knowledge on the main elements (C, N, O, and S) and other biocompounds that constitute them, whether structural or bioproducts. Regarding *Desmodesmus subspicatus,* the compositional mapping with the use of EDS revealed the main dispersion elements, such as carbon (51.0 %), oxygen (38.2 %), aluminum (6.6 %), nitrogen (4.5 %), sulfur (3.2 %), phosphor (0.6 %), and sodium (0.4 %) – the elemental composition of the latter ones was below 1.0 %. The carbon source used by DS can be in the form of either inorganic carbon (CO_2), or organic one (glucose, acetate, among others) for the production of fatty acids, hence, lipids, whose amount in each cell is different among the diverse microalgae species available [81] – the higher the carbon percentage, the better the thermal process of the sample. Among its main advantages are low carbon dioxide emissions to the atmosphere, contributing to reductions in both global warming and greenhouse effect, and availability of carbon sources to be used as feedstock for the biofuels production [79].

However, regarding *Pediastrum boryanum*, the order of the major

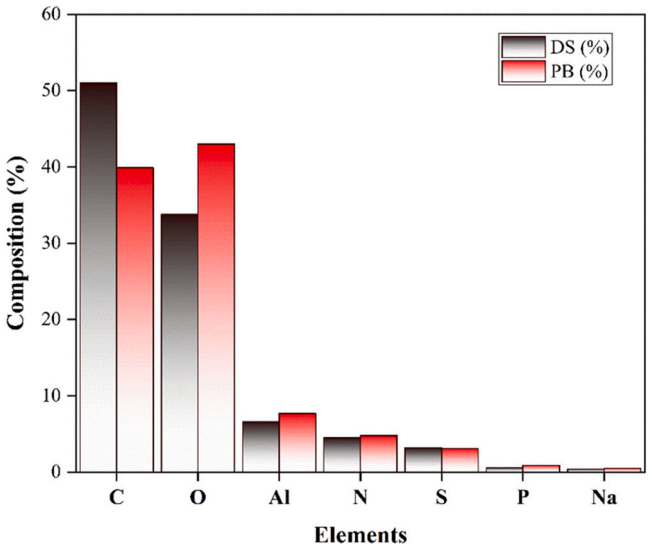

Fig. 8. Percentage of the main elements (organic, inorganic, and metallic ones) obtained by EDS for *Desmodesmus subspicatus* (DS) and *Pediastrum boryanum* (PB) samples.

dispersion elements was oxygen (43.0 %), carbon (39.9 %), aluminum (7.7 %), nitrogen (4.8 %), sulfur (3.1 %), phosphor (0.9 %), and sodium (0.5 %). The large quantity of oxygen atoms in the sample suggests the existence or formation of a large amount of oxides, hence, possible active sites in those microalgae, which are responsible for the complex reactions of biofuels production by thermochemical processes [76], or even the formation of corrosive agents for walls of ovens and/or furnaces, when those microalgae are applied in real thermal processes [26]. Moreover, the large quantity of carbon in the species composition is a strong indicator for the production of different biofuels (solid, liquid, and/or gaseous) by several thermochemical processes (combustion, pyrolysis, gasification, and/or oxy-fuel combustion).

3.9. X-ray diffraction (XRD)

Fig. 9 shows the XRD pattern for DS and PB samples.

The XRD measurements regarding *Desmodesmus subspicatus* (DS) and *Pediastrum boryanum* (PB) aimed at investigating the formation of crystalline and/or amorphous regions in the dry biomass samples. The diffractograms (Fig. 9) show a high predominance of the crystalline region, with 2θ ≈ 18.45°, and 30.29° for the two species. Such an amorphous structure may be related to the predominance of hemicellulose and less cellulose in the carbohydrates that form the cellular walls of some microalgae (e.g., *chlorophyceae* [82]). More intense and slender peaks were observed at 2θ ≈ 30.29° and 30.01° for DS and PB, respectively, which are probably associated with the formation of crystalline regions in the dry biomasses, as in *Spirulina platensis* [83]. The authors also reported a predominance of the amorphous region, with (2θ) 20.05° maximum value and a more pronounced peak, i.e., crystalline, at 2θ ≈ 28.5°, showing a PPB (protein by penicilina bond)-type protein crystallized in the microalgae drying treatment and employed as dehydrated powder for food supplementation [84].

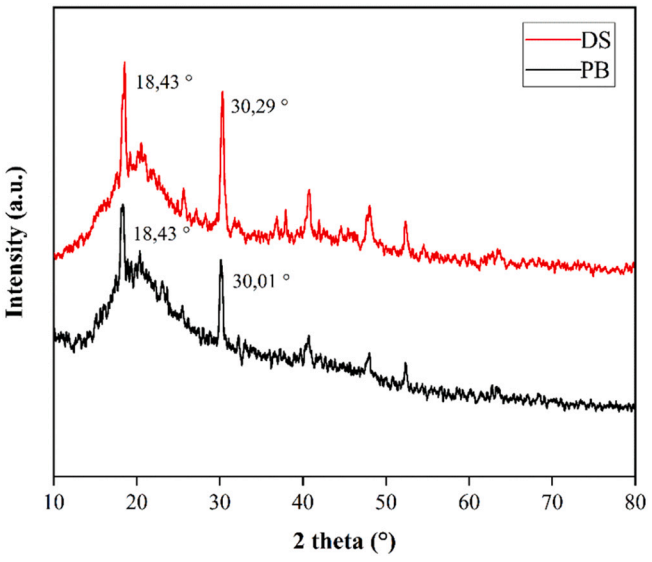

Fig. 9. X-ray diffraction for *Desmodesmus subspicatus* (DS) and *Pediastrum boryanum* (PB) samples.

The material's crystallinity index of cellulose (%CI) can be estimated from the width of the peaks collected in the XRD spectra. More intense and narrower peaks show a high crystallinity degree, whereas larger ones show a higher amount of amorphous region of the material [85]. The %CI obtained for the microalgae were 22.54 % for DS and 28.82 % for PB. Regarding the breakdown of intra and interchain hydrogen bonds, the crystalline degree for the lignocellulosic material is suitable for the presence of celullose, whose structure is highly crystalline; on the other hand, the components of hemicellulose and lignin are amorphous [86]. *Spirulina platensis* showed 19.08 % CI, hence, higher amorphism (80.92 %) [87], which are, respectively, lower and higher values than the ones from the present study.

According to Lee et al. [88], the pretreatment of an algal biomass is a limiting and more costly stage during the bioenergetic production process due to the complex cellular wall composition. However, the stage is highly required for minimizing the crystallinity degree of the cellulosic matrix, increasing the surface area and solubility of sugars, and improving the substrate digestibility [60]. Therefore, celullose and other polysaccharides (e.g., amide) are susceptible to hydrolysis, i.e., breakdown of sugars by physical, chemical, and/or biological treatments. The production of third-generation bioethanol requires a hydrolysis process in the exposition of micro and macrocomponents; consequently, the microalgae cellular wall is the main structure to be depolymerized for the extraction of several polysaccharides [89]. The acid treatment then works as a catalyst and the glycosidic linkages of the molecules are cleaved. At the end of the process, any addition or dilution of water will lead to a fast rupture of the hydrolyzed substrate in the constituent monosaccharides [90].

The X-ray patterns of DS and PB samples were very similar, since a large part of the peaks coincided. Moreover, the relative intensity of the diffraction peaks of the microalgae was reduced, probably due to a slight amorphization in the respective structures, which might have caused some distortion in the crystalline network [91].

3.10. Inductively coupled plasma optical emisson spectrometer (ICP-OES)

According to Fig. 10, the elemental composition of the biomass of *Desmodesmus subspicatus* (DS) and *Pediastrum boryanum* (PB) is mostly comprised of aluminum (Al) – 75.0 % on average. Iron (Fe < 5.0 %), found in the two samples, is also highly important for the algae cell, since its deficiency can limit a higher photosynthetic acitivity, with a reduced presence of chlorophyll, hence, an inhibition in the microalgae cultivation [66].

The different microalgae species are known to require some essential nutrients for their development and primarily composed of the following macronutrients: C, N, O, H, P, Ca, Mg, S, and K. Regarding micronutrients, they usually require Fe, Mn, Cu, Mo, and Co, obtained from the cultivation medium, i.e., WC (*Walter Culture*) [21]. Such additional information on the inorganic and metallic chemical composition of the two species was acquired only through the aforementioned technique.

Van Dam et al. [92] cultivated *Chlorella vulgaris* in a residual

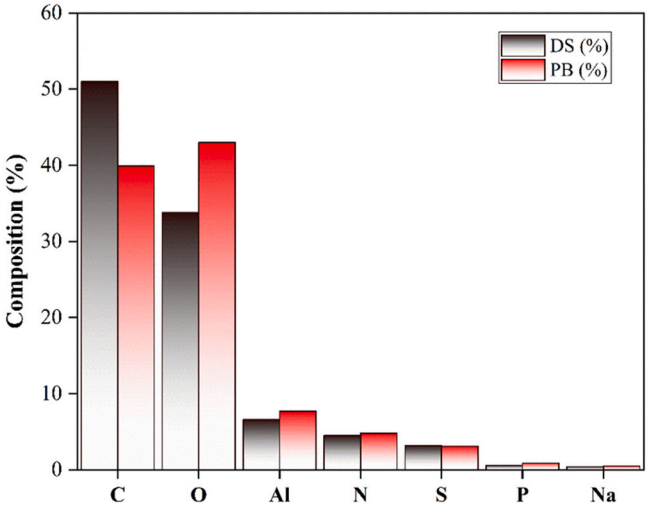

Fig. 10. Elemental composition of the two biomass species evaluated by ICP-OES (%).

hydroponic solution and analyzed its elemental composition by ICP-OES. The values found were 320.0 mg g^{-1} and 23.6 mg g^{-1} for iron (Fe) and zinc (Zn), respectively, which were lower than those for the same elements reported in the present study, namely 1706.0 mg g^{-1} and 46.0 mg g^{-1} for PB, and 1116.0 mg g^{-1} and 42.0 mg g^{-1} for DS. Such a difference may be related to the potential of the microalgae cells for adsorbing and absorbing nutrients from different cultivation media, since the nutritional solution for the hydroponic cultivation is rich in nutrients, including Fe and Zn [93].

Compositions of the cultivation medium are important for defining the composition of bioactives for specific purposes in the bioprospection of microalgae. Trace elements or oligoelements are essential in the functioning of algal metabolism; their lack or excess can alter the production of algal biomass and some bioactives. Cultivations with restriction in the amount of phosphor (P) and nitrogen (N) can lead to cellular stress, thus decreasing the protein content and accumulating lipids in the cellular content [94]. An increase in the lipid percentage of the microalgae makes it a potential candidate for the extraction of essential oils and production of by-products (e.g., biofuels, biodiesel, and biooil) [95,96].

3.11. Calorimetry analysis (HHV)

Heating value is an important parameter for defining the effective use of biofuels in real thermal processes [97]. The Higher Heating Value (HHV) obtained for *Pediastrum boryanum* (17.58 ± 0.03 MJ kg^{-1}) and *Desmodesmus subspicatus* (18.62 ± 0.03 MJ kg^{-1}), compared to the values found for *Oedogonium sp* (16.13 MJ kg^{-1}), *Scenedesmus* sp. (21.10 MJ kg^{-1}), *Chlorella vulgaris* (22.06 MJ kg^{-1}), and *Spirulina* (23.10 MJ kg^{-1}) [98,99], proved satisfactory, within an acceptable range for algal biomass, and indicated the high potential of the two species for thermoconversion in bioenergy.

Cristóbal et al. [100] stated microalgae biomass generally shows a higher carbon content and lower oxygen concentration when compared to traditional crop biomasses due to the high amount of energy released when C—C linkages are broken. Such an increase in carbon content directly corresponds to a rise in biofuel energy content [101]. Jamilatun et al. [102] studied the biooil composition of biomass *Spirulina platensis* (SP) and *Spirulina platensis residue* (SPR) after biooil extraction and observed their heating values (32.04 MJ kg^{-1} and 25.70 MJ kg^{-1}, respectively) were similar to those of crude oil (18.85 MJ kg^{-1}) and biooil (26.12 MJ kg^{-1}), reaffirming the promising values presented in the present study for the two microalgae species.

4. Conclusions

This study analyzed the cultivation of two microalgae species (*Pediastrum boryanum* and *Desmodesmus subspicatus*) through growth curve, total physicochemical characterization, and thermal behavior. The several techniques employed proved both species are highly relevant for the understanding of their biotechnological potential for the prodution of clean and renewable biofuels and/or bioenergy, due to the high heating value, composition of fatty acids, lipids, carbohydrates, proteins, and/or condensable and non-condensable combustion gases, which can directly influence the oxidative degradation process of the algal feedstock. However, some socioeconomic aspects must also be considered during the biotechnological process of bioenergy generation.

CRediT authorship contribution statement

G.S.S. Jacinto: conceptualization, methodology, validation, formal analysis, investigation, writing (original draft/review & editing), textual analysis. **G. Cruz**: conceptualization, methodology, investigation, resources, supervision, validation, writing (review & editing), textual analysis. **A.A. Cabral**: resources, supervision, writing (review & editing), textual analysis. **G.V.P. Bezerra**: methodology, textual analysis. **R. R. Peña Garcia**: resources, writing review, textual analysis. **U.N. Magalhães**: resources, writing review, textual analysis. **W.C. Gomes**: resources, supervision, writing review, textual analysis.

Declaration of competing interest

The authors declare they have no known competing financial interests or personal relationships that might have influenced the work described herein.

Data availability

Data will be made available on request.

Acknowledgments

The authors gratefully acknowledge the financial support of Brazilian research funding agencies, FAPEMA (Maranhão Foundation for Scientific Research and Technological Development - Processes no. 05516/19, 01661/21, 00013/22, and 06776/22), as well as the professional and technical support from the following universities: Federal University of Maranhão - UFMA, Federal Institute of Education, Science, and Technology of Maranhão - IFMA, and Federal Rural University of Pernambuco - UFRPE.

Appendix A. Supplementary data

Supplementary data to this article can be found online at https://doi.org/10.1016/j.algal.2023.103266.

References

[1] R.H. Wijffels, M.J. Barbosa, An outlook on microalgal biofuels, Science 329 (2010) 796–799, https://doi.org/10.1126/science.1189003.
[2] E. Atabani, S. Shobana, M.N. Mohammed, G. Uğuz, G. Kumar, S. Arvindnarayan, A. Muhammad, H.A.M. Ala'a, Integrated valorization of waste cooking oil and spent coffee grounds for biodiesel production: blending with higher alcohols, FT–IR, TGA, DSC and NMR characterizations, Fuel Length Article 244 (2019) 419–430, https://doi.org/10.1016/j.fuel.2019.01.169.
[3] G.M. Elrayies, Microalgae: prospects for greener future buildings, Renew. Sustain. Energy Rev. 81 (2018) 1175–1191, https://doi.org/10.1016/j.rser.2017.08.032.
[4] M. Maaz, M. Yasin, M. Aslam, G. Kumar, A.E. Atabani, M. Idrees, A. Fatima, J. Farrukh, A. Rizwan, K.A. Asim, L. Geoffroy, H. Marc, K. Jeonghwan, Anaerobic membrane bioreactors for wastewater treatment: novel configurations, fouling control and energy considerations, Bioresour. Technol. 283 (2019) 358–372, https://doi.org/10.1016/j.biortech.2019.03.061.

[5] A. Khalid, A. Muhammad, A. Muhammad, F. Abrar, K.A. Laeeq, A. Faisal, L. Moonyong, K. Jeonghwan, J. Nulee, C. Seop, B.A. Bazmi, Y. Muhammad, Membrane separation processes for dehydration of bioethanol from fermentation broths: recent developments, challenges, and prospects, Renew. Sustain. Energy Rev. 105 (2019) 427–443, https://doi.org/10.1016/j.rser.2019.02.002.

[6] S. Marco, M. Alan, E. Herman van den, K. Henk, C. Piet, M. Pieter van der, *Chlamydomonas eugametos* (*chlorophyta*) stores phosphate in polyphosphate bodies togetherwith calcium, J. Phycol. 32 (2016) 402–409, https://doi.org/10.1111/j.0022-3646.1996.00402.x.

[7] Z. Zhang, J. Hairui, G. Guiping, X. Zhang, T. Tianwei, Synergistic effects of oleaginous yeast *Rhodotorula glutinis* and microalga *Chlorella vulgaris* for enhancement of biomass and lipid yields, Bioresour. Technol. 164 (2014) 93–99, https://doi.org/10.1016/j.biortech.2014.04.039.

[8] N. Arora, L.M.L. Laurens, N. Sweeney, V. Pruthi, K.M. Poluri, P.T. Pienkos, Elucidating the unique physiological responses of halotolerant *Scenedesmus* sp. cultivated in sea water for biofuel production, Algal Res. 37 (2019) 260–268, https://doi.org/10.1016/j.algal.2018.12.003.

[9] S. Sivagnanam, L. Peter, S. Ramachandran, I. Aran, K. Balu, C. Pablo, *Scenedesmus* sp. strain SD07 cultivation in municipal wastewater for pollutant removal and production of lipid and exopolysaccharides, Environ. Res. 218 (2023), 115051, https://doi.org/10.1016/j.envres.2022.115051.

[10] P. Gaurav, D.P. Yadav, G. Ashish, ResNeXt convolution neural network topology-based deep learning model for identification and classification of *Pediastrum*, Algal Res. 48 (2020), 101932, https://doi.org/10.1016/j.algal.2020.101932.

[11] E. Houda, I. Tasneema, M.O. Victor, M.R. Navid, Microalgal biofilms: towards a sustainable biomass production, Algal Res. 72 (2023), 103124, https://doi.org/10.1016/j.algal.2023.10312.

[12] S.A. Mariana, B.H. Gabriel, C.B. Carolina, M.A.F. Luiz, B.G. Reinado, Heterotrophic growth of green microalgae *Desmodesmus subspicatus* in ethanol distillation wastewater (vinasse) and lipid extraction with supercritical CO_2, J. Chem. Technol. Biotechnol. 92 (2017) 573–579, https://doi.org/10.1002/jctb.5035.

[13] P. Haiyan, Z. Lijie, B.J. Michael, J. Liqun, L. Xiao, M. Chunxia, Y. Zhigang, W. Xiaodong, C. Shuaiqi, L. Wen-Feng, Highly efficient harvesting and lipid extraction of limnetic *Chlorella sorokiniana* SDEC-18 grown in seawater for microalgal biofuel production, Algal Res. 66 (2022) 102813, https://doi.org/10.1016/j.algal.2022.102813.

[14] M.O. Victor, I. Tasneema, M.R. Navid, E. Houda, The potential of coupling wastewater treatment with hydrocarbon production using *Botryococcus braunii*, Algal Res. (2023), 103214, https://doi.org/10.1016/j.algal.2023.103214.

[15] M. Huesemann, S. Edmundson, S. Gao, S. Negi, T. Dale, A. Gutknecht, H. E. Daligault, K.C. Carol, J. Freeman, T. Kern, S.R. Starkenburg, C.D. Gleasner, W. Louie, R. Kruk, S. McGuire, DISCOVR strain pipeline screening – part I: maximum specific growth rate as a function of temperature and salinity for 38 candidate microalgae for biofuels production, Algal Res. 71 (2023) 102996, https://doi.org/10.1016/j.algal.2023.102996.

[16] Q. Shasha, W. Zhongzhong, H. Yuansheng, L. Ji, Z. Xinmin, S.B. Dagmar, Selective enrichment of auto-floating microalgae for wastewater bioremediation and biofuel/bioproduct production, Algal Res. 69 (2023) 102911, https://doi.org/10.1016/j.algal.2022.102911.

[17] S. Chinnasamy, B. Ramakrishnan, A. Bhatnagar, K.C. DAS, Biomass production potential of a wastewater alga *Chlorella vulgaris* ARC 1 under elevated levels of CO_2 and temperature, Int. J. Mol. Sci. 10 (2019) 518–532, https://doi.org/10.3390/ijms10020518.

[18] M.J. Joshua, F.J. Kevin, S.J. Robin, Rapid determination of bulk microalgal biochemical composition by Fourier-transform infrared spectroscopy, Bioresour. Technol. 148 (2013) 215–220, https://doi.org/10.1016/j.biortech.2013.08.133.

[19] D. Vamvuka, S. Sfakiotakis, Effects of heating rate and water leaching of perennial energy crops on pyrolysis characteristics and kinetics, Renew. Energy 36 (2011) 2433–2439, https://doi.org/10.1016/j.renene.2011.02.013.

[20] K. Chiu-Mei, C. Tsai-Tu, L. Tsung-Hsien, K. Chiem-Ya, L. Jinn-Tsyy, C. Jo-Shu, L. Chih-Sheng, Cultivation of *Chlorella* sp. GD using piggery wastewater for biomass and lipid production, Bioresour. Technol. 194 (2015) 326–333, https://doi.org/10.1016/j.biortech.2015.07.026.

[21] R.R.L. Guillard, Culture of phytoplankton for feeding marine invertebrates, in: W. L. Smith, M.H. Chanley (Eds.), Culture of Marine Invertebrate Animals, 1975, pp. 29–60, https://doi.org/10.1007/978-1-4615-8714-9_3.

[22] P.C.C. Aline, F.T. Juliana, T.F. Luciane, G. Mariliz, Study of a consortium of microalgae in the removal of nutrients from tannery effluents, UERGS Sci. Electron. J. 4 (2017) 743–752, https://doi.org/10.21674/2448-0479.34.743-752.

[23] N.G. Emeka, P.A. David, L.W. Damian, A. Kamal, M.R. Navid, Light management technologies for increasing algal photobioreactor efficiency, Algal Res. 39 (2019), 101433, https://doi.org/10.1016/j.algal.2019.101433.

[24] C.Y. Sook, P.N.M. Krishna, W.Y. Ta, R.E. Mavinakere, P. Siew-Moi, J.C. Joon, R. N. Ramakrishnan, Starch-based flocculant outperformed aluminium sulfate hydrate and polyaluminium chloride through effective bridging for harvesting acicular microalga *Ankistrodesmus*, Algal Res. 29 (2018) 343–353, https://doi.org/10.1016/j.algal.2017.11.001.

[25] Z. Liandong, H. Tianyi, L. Shuangxi, N.K. Yohanes, L. Baishan, C. Jun, H. Erkki, Effects of operating parameters on algae *Chlorella vulgaris* biomass harvesting and lipid extraction using metal sulfates as flocculants, Biomass Bioenergy 132 (2020), 105433, https://doi.org/10.1016/j.biombioe.2019.105433.

[26] A.V.S. Silva, D.A. Mortari, C.C. Conconi, F.M. Pereira, G. Cruz, Investigation of the combustion process of fish scales from Northeast Brazil in a tubular drop furnace (DTF), Environ. Sci. Pollut. Res. 29 (2022) 67270–67286, https://doi.org/10.1007/s11356-022-20643-x.

[27] L. Guy, K. Sharon, L. Varda, E. Benjamim, M. Ayala, I. Tal, T. Yaakov, A. Noam, S. Gadi, The desert green algae *Chlorella ohadii* thrives at excessively high light intensities by exceptionally enhancing the mechanisms that protect photosynthesis from photoinhibition, Plant J. 106 (2021) 1260–1277, https://doi.org/10.1111/tpj.15232.

[28] C.T. Yu, W.H. Chen, L.C. Men, W.S. Hwang, Structure characteristics changes of rice straw treated with boiled acid solution, Ind. Crop. Prod. 29 (2009) 308–315, https://doi.org/10.1016/j.indcrop.2008.06.005.

[29] American Society for Testing and Materials – ASTM E711, Standard Test Method for Gross Calorific Value of refuse – Derived Fuel by the Bomb Calorimeter, 2023.

[30] K. Ranglová, G.E. Lakatos, J.A.C. Manoel, Rapid screening test to estimate temperature optima for microalgae growth using photosynthesis activity measurements, Folia Microbiol. 64 (2019) 615–625, https://doi.org/10.1007/s12223-019-00738-8.

[31] K.S. Kuan, L.Y. Sze, O.W. Chien, F. Xiaothing, M. Xiaothing, L.C. Tau, S.L. Pau, Recent advances in biorefinery of astaxanthin from *Haematococcus pluvialis*, Bioresour. Technol. 288 (2019), 1216006, https://doi.org/10.1016/j.biortech.2019.121606.

[32] W. Suzana, I. Ani, Y.M. Norordin, K.H.H. Nor, S.R.M. Sitti, Optimization of the ionic liquid-microwave assisted one-step biodiesel production process from wet microalgal biomass, Energ. Conver. Manage. 171 (2018) 1397–1404, https://doi.org/10.1016/j.enconman.2018.06.083.

[33] S.R. Raquel, A.Q.F. Ofélia, M.L. José, C.M. Ricardo, Cultivation of *Spirulina maxima* in medium supplemented with sugarcane vinasse, Bioresour. Technol. 204 (2016) 38–48, https://doi.org/10.1016/j.biortech.2015.12.077.

[34] Y. Xiaogang, Y. Libin, Z. Xuefei, Z. Yalei, Sustainability and carbon neutrality trends for microalgae-based wastewater treatment: a review, Environ. Res. 209 (2022), 112860, https://doi.org/10.1016/j.envres.2022.112860.

[35] G.E.B. Montalvo, V. Thomaz-Soccol, L.P.S. Vandenberghe, J.C. Carvalho, C. B. Faulds, E. Bertrand, M.R.M. Prado, S.J.R. Bonatto, R.C. Soccol, *Arthrospira maxima* OF15 biomass cultivation at laboratory and pilot scale from sugarcane vinasse for potential biological new peptides production, Bioresour. Technol. 273 (2019) 103–113, https://doi.org/10.1016/j.biortech.2018.10.081.

[36] M.S. Daniela, V.T. Raunel, B.C.A. Mario, M. Alfredo, Culturing *Neochloris oleoabundans* microalga in a nitrogen limited, heterotrophic fedbatch system to enhance lipid and carbohydrate accumulation, Algal Res. 5 (2014) 61–69, https://doi.org/10.1016/j.algal.2014.05.006.

[37] P. Chiranjeevi, M.S. Venkata, Critical parametric influence on microalgae cultivation to maximize biomass growth with simultaneous lipid productivity, Renew. Energy 98 (2016) 64–71, https://doi.org/10.1016/j.renene.2016.03.063.

[38] G. Stephanie, S. Micha, W. Ramona, M. Daniel, Consumer oriented product development: the conceptualization of novel food products based on spirulina (*Arthrosporic platensis*) and resulting consumer expectations, J. Food Qual. (2018), https://doi.org/10.1155/2018/1919482.

[39] G. Biyensa, P.F. Ester, C. Stefania, C. Valeria, C. Giuseppe, Manure anaerobic digestion effects and the role of pre-and post-treatments on veterinary antibiotics and antibiotic resistance genes removal efficiency, Sci. Total Environ. 721 (2020), 137532, https://doi.org/10.1016/j.scitotenv.2020.137532.

[40] H. Fida, S. Shah, Z. Syed, A. Habib, A. Samar, A. Aubshait, A. Haya, A. Laref, A. Manikandan, A. Kusuma, S. Heri, S. Munawar, Microalgae an ecological and sustainable option for wastewater treatment: application of biomass in the production of biofuels and biofertilizers. A review, Renew. Sustain. Energy Rev. 137 (2021), 110603, https://doi.org/10.1016/j.rser.2020.110603.

[41] M. Marzieh, S. Ali, S. Vahideh, Effects of heavy metal contamination on river water quality due to release of industrial effluents, J. Clean. Prod. 277 (2020), 123380, https://doi.org/10.1016/j.jclepro.2020.123380.

[42] G. Abhishek, S. Poonam, A.A. Faiz, S. Bhaskar, B. Faizal, Biodiesel synthesis from microalgal lipids using tungstated zirconia as a heterogeneous acid catalyst and its comparison with homogeneous acid and enzyme catalysts, Food Chem. 187 (2017) 180–188, https://doi.org/10.1016/j.fuel.2016.09.053.

[43] P. Shu-Yuan, T. Cheng-Yen, L. Cheng-Wuing, W. Sheng-Wei, K. Hyunook, F. Chihhao, Anaerobic co-digestion of agricultural waste towards a circular bioeconomy, Iscience 24 (2021), 102704, https://doi.org/10.1016/j.isci.2021.102704.

[44] S.K. Ramesh, K.S. Young, Carotenoid extraction methods: a review of recent developments, Food Chem. 240 (2018) 90–103, https://doi.org/10.1016/j.foodchem.2017.07.099.

[45] F. Ferreira, A.P. Soares, C.M. Silva, M. Costa, Evaluation of thermochemical properties of raw and extracted microalgae, Energy 92 (2015) 365–372, https://doi.org/10.1016/j.energy.2015.04.078.

[46] T. Shahi, B. Beheshti, A. Zenouzi, M. Almasi, Bio-oil production from residual biomass of microalgae after lipid extraction: the case of *Dunaliella Sp*, Biocatal. Agric. Biotechnol. 23 (2020) 101494, https://doi.org/10.1016/j.bcab.2020.101494.

[47] D. Thomas, B.K. Amit, A.J. Willian, G. Royston, P.K. Jon, D.P. Andrew, The metabolic responses of eukaryotic microalgae to environmental stress limit the ability of FT-IR spectroscopy to identify species, Algal Res. 11 (2015) 148–155, https://doi.org/10.1016/j.algal.2015.06.009.

[48] V. Challagulla, K.B. Walsh, P. Subedi, Microalgal fatty acid composition: rapid assessment using near-infrared spectroscopy, J. Appl. Phycol. 28 (2015) 85–94, https://doi.org/10.1007/s10811-015-0533-5.

[49] Z. Gojkovic, A. Shchukarev, M. Ramstedt, C. Funk, C. Cryogenic X-ray photoelectron spectroscopy determines surface composition of algal cells and

gives insights into their spontaneous sedimentation, Algal Res. 47 (2020), 101836, https://doi.org/10.1016/j.algal.2020.101836.
[50] G. Bataller, S.C. Capareda, A rapid and non-destructive method for quantifying biomolecules in *Spirulina platensis* via Fourier transform infrared-attenuated total reflectance spectroscopy, Algal Res. 32 (2018) 341–352, https://doi.org/10.1016/j.algal.2018.04.023.
[51] S. Christian, R. Jakob, W. Martina, O.G. Jose, S. Volker, M. Sabine, A one-stage cultivation process for lipid- and carbohydrate-rich biomass of *Scenedesmus obtusiusculus* based on artificial and natural water sources, Bioresour. Technol. 218 (2016) 498–504, https://doi.org/10.1016/j.biortech.2016.06.109.
[52] M.S.C. Eduardo, M.S.R. Mariano, H. Nestor, V.S. Antonio, Microalgae pyrolysis under isothermal and non-isothermal conditions, Algal Res. 51 (2020), 102031, https://doi.org/10.1016/j.algal.2020.102031.
[53] V. Sergey, B.K. Alan, F. Loic, K. Nobuyoshi, M. Elena, M.P.A. Luis, S. Nicolas, ICTAC kinetics committee recommendations for multi-step kinetics analysis, Thermochim. Acta 686 (2020), 178597, https://doi.org/10.1016/j.tca.2020.178597.
[54] D. Federica, M. Mauro, F. Francesca, F. Javier, O. Alessandro, S. Aimaro, P. Alberto, Thermogravimetric characterization and kinetic analysis of *Nannochloropsis* sp. and *Tetraselmis* sp. microalgae for pyrolysis, combustion and oxy-combustion, Energy 217 (2021), 119394, https://doi.org/10.1016/j.energy.2020.119394.
[55] J. Martín-Juárez, G. Markou, K. Muylaert, A. Lorenzo-Hernando, S. Bolado, Breakthroughs in bioalcohol production from microalgae: solving the hurdles, in: Microalgae-Based Biofuels and Bioproducts: From Feedstock Cultivation to End Products, 2017, pp. 183–207, https://doi.org/10.1016/B978-0-08-101023-5.00008-X.
[56] L.C. Vera, M. Mandy, A.M. Antonio, K.H. Svein, B. Simon, R.L. Amparo, S. M. Marta, Valorization of alginate-extracted seaweed biomass for the development of cellulose-based packaging films, Algal Res. 61 (2022), 102576, https://doi.org/10.1016/j.algal.2021.102576.
[57] C. Jieteng, Z. Weishun, G. Jing, L. Yunxue, P. Yifan, L. Juyan, C. Hao, Physicochemical properties and anti-oxidation activities of ulvan from *Ulva pertusa* Kjellm, Algal Res. 55 (2021), 102269, https://doi.org/10.1016/j.algal.2021.102269.
[58] G. Basil, P. Imran, D. Chahana, C. Kaumeel, P. Chetan, G. Tonmoy, M. Sandhya, Effects of different media composition, light intensity and photoperiod on morphology and physiology of freshwater microalgae *Ankistrodesmus falcatus* – a potential strain for biofuel production, Bioresour. Technol. 171 (2015) 367–374, https://doi.org/10.1016/j.biortech.2014.08.086.
[59] W. Lin, P. Bishu, S. Jianchun, X. Juan, H. Qiuhui, Antioxidant activity of *Spirulina platensis* extracts by supercritical carbon dioxide extraction, Food Chem. 105 (2007) 36–41, https://doi.org/10.1016/j.foodchem.2007.03.054.
[60] G. Cruz, C.E.M. Braz, I. Avila, P.M. Crnkovic, Physico-chemical properties of brazilian biomass: potential applications as renewable energy source, Afr. J. Biotechnol. 17 (2018), https://doi.org/10.5897/AJB2017.16296.
[61] A. Marcilla, A. Gómez-Siurana, C. Gomis, E. Chápuli, M.C. Catalá, F.J. Valdés, Characterization of microalgae species through TGA/FTIR analysis: application to *Nannochloropsis* sp, Thermochim. Acta 484 (2009) 41–47, https://doi.org/10.1016/j.tca.2008.12.005.
[62] G. Cruz, P.M. Crnkovic, PM, Assessment of the physical-chemical properties of residues and emissions generated by biomass combustion under N_2/O_2 and CO_2/O_2 atmospheres in a Drop Tube Furnace (DTF), J. Therm. Anal. Calorim. 138 (2019) 401–415, https://doi.org/10.1007/s10973-019-08238-0.
[63] S. Mandal, N. Mallick, *Scenedesmus obliquus* as a potential source for biodiesel production, Appl. Microbiol. Biotechnol. 84 (2009) 281–291, https://doi.org/10.1007/s00253-009-1935-6.
[64] Y. Xu, Y. Hu, Y. Peng, L. Yao, Y. Dong, B. Yang, Catalytic pyrolysis and liquefaction behavior of microalgae for bio-oil production, Bioresour. Technol. 300 (2020), 122665, https://doi.org/10.1016/j.biortech.2019.122665.
[65] J. Fermoso, T. Corbet, F. Ferrara, A. Pettinau, E. Maggio, A. Sanna, Synergistic effects during copyrolysis and cogasification of volatile bituminous coal with microalgae, Energy Convers. Manag. 164 (2018) 399–409, https://doi.org/10.1016/j.enconman.2018.03.023.
[66] Z. Wu, J. Zhang, B. Zhang, W. Guo, G. Yang, B. Yang, Synergistic effects of co-pyrolysis of the main component of lignocellulosic biomass with low-grade charcoal: online and offline analysis on product distribution and kinetic characteristics, Appl. Energy 276 (2020), https://doi.org/10.1016/j.apenergy.2020.115461.
[67] J. Li, Y. Qiao, P. Zong, C. Wang, Y. Tian, S. Qin, Thermogravimetric analysis and isoconversional kinetic study of biomass pyrolysis derived from land, coastal zone, and marine, Energy Fuel 33 (2019) 3299–3310, https://doi.org/10.1021/acs.energyfuels.9b00331.
[68] R.K. Mishra, K. Mohanty, Kinetic analysis and pyrolysis behavior of residual biomass in relation to its bioenergy potential, Bioresour. Technol. 311 (2020) 12348, https://doi.org/10.1016/j.mset.2021.03.003.
[69] Y. Chun-Yen, A. Kuei-Ling, L. Rifka, C. Duu-Jong, C. Jo-Shu, Cultivation, photobioreactor design and harvesting of microalgae for biodiesel production: a critical review, Bioresour. Technol. 102 (2019) 71–81, https://doi.org/10.1016/j.biortech.2010.06.159.
[70] W.J. Katharina, T. Andreas, K. Mirco, S. Herbet, P. Clemens, R. Markus, Chemical composition and nutritional characteristics for ruminants of the microalgae *Chlorella vulgaris* obtained under different growing conditions, Algal Res. 38 (2019), 101385, https://doi.org/10.1016/j.algal.2018.101385.
[71] P. Jainedra, S.S. Arun, R. Richa, K.K. Vinod, S. Vidya, A. Hassen, S.P. Rajeshwar, Screening and partial purification of photoprotective pigment scytonemin from cyanobacterial crusts dwelling on the historical monuments in and around Varanasi, Microbiol. Res. 8 (2017) 6559, https://doi.org/10.4081/mr.2017.6559.
[72] Z. You, X. Xiaojie, Machine learning glass transition temperature of polymers, Heliyon 6 (2020), e05055, https://doi.org/10.1016/j.heliyon.2020.e05055.
[73] R.S.S. Sidra, C. Muhammad, S. Muhammad, M. Nawshad, K. Shahzad, M. Khaliq, K.L. Asim, G. Moinuddin, J. Farrunk, A. Muhammad, Facile CO_2 separation in composite membranes, Chem. Eng. Technol. 42 (2019) 30–44, https://doi.org/10.1002/ceat.201700653.
[74] S. Suh, C.G. Lee, Photobioreactor engineering: design and performance, Biotechnol. Bioprocess Eng. 8 (2003) 313–321, https://doi.org/10.1007/BF02949274.
[75] M. Kanzy, N.F. Nasr, H.A.M. El-Shazly, O.S. Barakat, Optimization of carotenoids production by yeast strains of *Rhodotorula* using salted cheese whey, Int. J. Curr. Microbiol. App. Sci. 4 (2015) 456–469. https://www.researchgate.net/publication/315927240.
[76] O.U. Patrick, W. Song, X. Lanlan, L. Sanxi, W. Jianye, Z. Linnan, Promotional effect of calcination temperature on structural evolution, basicity, and activity of oil palm empty fruit bunch derived catalyst for glycerol carbonate synthesis, Energ. Conver. Manage. 179 (2019) 192–200, https://doi.org/10.1016/j.enconman.2018.10.013.
[77] L.V. Junping, Z. Fei, F. Jia, L. Qi, N. Fangru, L. Xudong, X. Shulian, The impact of particulate and soluble organic matter on physicochemical properties, Algal Res. 51 (2020), 102064, https://doi.org/10.1016/j.algal.2020.102064.
[78] P.R.C.F. Ribeiro, S.S.O. Silva, M.R. Nascimento, S.A. Soares, F.M.T. Luna, C. L. Cavalcante, Tribological properties of bio-based lubricant basestock obtained from pequi oil (*Caryocar brasiliensis*), J. Braz. Soc. Mech. Sci. Eng. 44 (2022) 51, https://doi.org/10.1007/s40430-021-03358-x.
[79] A.G.P. Alvarenga, M.G.D. Morais, J.A.V. Costa, Development of polymeric nanospheres for addition of microalgae biomass, Multidiscip. J. Educ. Environ. 2 (2021) 23, https://doi.org/10.51189/rema/1350.
[80] C. Breil, V.M. Maryline, Z. Thomas, K. Wenner, C. Farid, "Bligh and dyer" and Folch methods for solid–liquid–liquid extraction of lipids from microorganisms. Comprehension of solvatation mechanisms and towards substitution with alternative solvents, Int. J. Mol. Sci. 18 (2017) 708, https://doi.org/10.3390/ijms18040708.
[81] F.S. Eshaq, M.N. Ali, M.K. Mohd, *Spirogyra* biomass a renewable source for biofuel (bioethanol) production, Int. J. Eng. Sci. Technol. 2 (2010) 7045–7054. https://www.researchgate.net/publication/50384251.
[82] A.C.C. Rodrigues, C.A. Henriques, J.L. Monteiro, Influence of Ni content on physico-chemical characteristics of Ni, Mg, Al-hydrotalcite like compounds, Mater. Res. 6 (2003) 563–568, https://doi.org/10.1590/S1516-14392003000400024.
[83] R.D. Andrei, M.I. Popa, F. Fajula, V. Hulea, Heterogeneous oligomerization of ethylene over highly active and stable Ni-AlSBA-15 mesoporous catalysts, J. Catal. 323 (2015) 76–84, https://doi.org/10.1016/j.jcat.2014.12.027.
[84] K.K. Jaiswal, V. Kumar, M.S. Vlashin, M. Nanda, Impact of glyphosate herbicide stress on metabolic growth and lipid inducement in *Chlorella sorokiniana* UUIND6 for biodiesel production, Algal Res. 51 (2020), 102071, https://doi.org/10.1016/j.algal.2020.102071.
[85] F. Peters, K. Schwarz, M. Epple, The structure of bone studied with synchrotron X-ray diffaction, X-ray absorption spectroscopy and thermal analysis, Thermochim. Acta 361 (2000) 131–138, https://doi.org/10.1016/S0040-6031(00)00554-2.
[86] A. Vo, F.M. Nicholas, F.J. Mary, C.Y. Lee, J.A. Cosman, C.A. Glynn, Z.O. Hassan, D. Perlstein, Identifying the protein interactions of the cytosolic iron-sulfur cluster targeting complex essential for its assembly and recognition of apo-targets, Biochemistry 57 (2018) 2349–2358, https://doi.org/10.1021/acs.biochem.7b00072.
[87] M.I. Khan, J.H. Shin, J.D. Kim, The promising future of microalgae: current status, challenges, and optimization of a sustainable and renewable industry for biofuels, feed, and other products, Microb. Cell Factories 17 (2018) 36, https://doi.org/10.1186/s12934-018-0879-x.
[88] S.Y. Lee, J.M. Cho, Y.K. Chang, Cell disruption and lipid extraction for microalgal biorefineries: a review, Bioresour. Technol. 244 (2017) 1317–1328, https://doi.org/10.1016/j.biortech.2017.06.038.
[89] B.E. Reiber, Opportunities for renewable bioenergy using microorganisms, Biotechnol. Bioeng. 100 (2008) 203–212, https://doi.org/10.1002/bit.21875.
[90] P.L. Show, M.S.Y. Tang, D. Nagarajan, T.C. Ling, C. Ooi, J. Chang, A holistic approach to managing microalgae for biofuel applications, Int. J. Mol. Sci. 18 (2017) 215, https://doi.org/10.3390/ijms18010215.
[91] A. Vasconcellos, J.B. Laurenti, A.H. Miller, D.A. Silva, F.R. Moraes, D.A. G. Aranda, Potential new biocatalysts for biofuel production: the fungal lipases of *Thermomyces lanuginosus* and *Rhizomucor miehei* immobilized on zeolitic supports ion exchanged with transition metals, Microporous Mesoporous Mater. 214 (2015) 166–180, https://doi.org/10.1016/j.micromeso.2015.05.007.
[92] R.A. Van Dam, A.J. Harford, S.A. Lunn, M.M. Gagnon, Identifying the cause of toxicity of a saline mine water, PLoS One 9 (2009), 106857, https://doi.org/10.1371/journal.pone.0106857.
[93] A. Mariajoseph, N. Punia, A. Velmurugan, A. Balasubramaniem, G.M. Innasi, B. Kathirvel, T.L.C. Nguyen, P. Arivalagan, V. Perumal, Phycoremediation of Arsenic and biodiesel production using green microalgae *Coelastrella* sp. M60 – an integrated approach, Fuel 333 (2023), 126427, https://doi.org/10.1016/j.fuel.2022.126427.
[94] L. Wang, B. Pan, J. Sheng, J. Xu, Q. Hu, Antioxidant activity of *Spirulina platensis* extracts by supercritical carbon dioxide extraction, Food Chem. 105 (2007) 36–41, https://doi.org/10.1016/j.foodchem.2007.03.054.

[95] P. Neeranuch, C. Benjamas, Integrated protein extraction with bio-oil production for microalgal biorefinery, Algal Res. 48 (2020), 101918, https://doi.org/10.1016/j.algal.2020.101918.
[96] M.C. Bruno, C. Ruben, L. Chantal, A. Pavel, L. Dorothée, G. Christople, Catalytic hydroconversion of HTL micro-algal bio-oil into biofuel over NiWS/Al_2O_3, Algal Res. 71 (2023), 103012, https://doi.org/10.1016/j.algal.2023.103012.
[97] S. Myrsini, K. Michael, *Chlorella vulgaris* as a green biofuel factory: comparison between biodiesel, biogas and combustible biomass production, Bioresour. Technol. 273 (2019) 237–243, https://doi.org/10.1016/j.biortech.2018.11.017.
[98] M.B. Iara, P.P.A.S. Alexia, S.A. Thiago, R.S. Natalia, Predicting the higher heating value of microalgae biomass based on proximate and ultimate analysis, Algal Res. 64 (2022), 102677, https://doi.org/10.1016/j.algal.2022.102677.
[99] P. Sulochana, T. Zlatan, S.R. Joel, L.C. Han, C.D. Nicholas, S.J. Peter, M. J. Gregory, Variation of the photosynthesis and respiration response of filamentous algae (*Oedogonium*) acclimated to averaged seasonal temperatures and light exposure levels, Algal Res. 74 (2023), 103213, https://doi.org/10.1016/j.algal.2023.103213.
[100] A. Cristóbal, R.G. Chasoy, J.M.R. Rosa, B. Germán, C. Isaac, R.A. Héctor, Growth kinetics and quantification of carbohydrate, protein, lipids, and chlorophyll of *Spirulina platensis* under aqueous conditions using different carbon and nitrogen sources. 126456, Bioresour. Technol. 346 (2022), 126456, https://doi.org/10.1016/j.biortech.2021.126456.
[101] L.A. Andrade, F.R.X. Batista, M.A.S. Barrozo, L.G.M. Vieira, Characterization and product formation during the catalytic and non-catalytic pyrolysis of the green microalgae *Chlamydomonas reinhardtii*, Renew. Energy 119 (2018) 731–740, https://doi.org/10.1016/j.renene.2017.12.056.
[102] S. Jamilatun, B. Rochmadib, A. Yuliestyanc, A. Budiman, Comparative analysis between pyrolysis products of *Spirulina platensis* biomass and its residues, Int. J. Renew. Energy Dev. 8 (2019) 133–140, https://doi.org/10.14710/ijred.8.2.133-140.